JOURNAL OF MATERIALS SCIENCE **40** (2005) 1717–1723

Fabrication, characterisation and application of (8 mol% Y_2O_3) ZrO_2 thin film on $Na_3Zr_2Si_2PO_{12}$ substrate for sensing CO_2 gas

L. WANG
School of Chemical Engineering and Biotechnology, Hebei Polytechnic University, Tangshan City 063009, People's Republic of China

L. PAN, J. SUN, Y. R. HONG
Department of Materials Science, University of Science and Technology Beijing, Beijing 10083, People's Republic of China

G. M. KALE*
Institute for Materials Research, University of Leeds, Leeds, LS2 9JT, UK
E-mail: g.m.kale@leeds.ac.uk

A planar type CO_2 gas sensor employing (8 mol% Y_2O_3) ZrO_2 (YSZ) thin film on $Na_3Zr_2Si_2PO_{12}$ (Nasicon) substrate with Na_2CO_3 as an auxiliary electrode has been fabricated and tested in laboratory environment between 700–900 K. The YSZ thin film was fabricated on Nasicon and alumina substrate using radio frequency (RF) magnetron sputtering. The film was examined using SEM and X-ray diffraction (XRD) after treating the Nasicon-YSZ bi-layer structure at 1300 K for 2 h. The results indicate that a crack free YSZ film was produced on Nasicon surface that was well bonded to the substrate. The conductivity of sputtered YSZ thin film measured by ac-impedance spectroscopy has been found to be higher than that of YSZ pellet by approximately half an order of magniture. The bi-electrolyte planar sensor displays rapid response ($t_{95} \leq 200$ s) to CO_2 compared to the tube type sensor ($t_{95} \leq 700$ s) and the measured open circuit voltage of the electrochemical CO_2 sensor has been found to be Nernstian at all temperatures.

1. Introduction

Combustion of fossil fuels is the major contributor of pollutants including gaseous oxides of carbon, nitrogen and sulphur such as CO_X ($X = 1, 2$), NO_X ($X = 1, 2$), SO_X ($X = 2, 3$) and non-methane volatile organic compounds (NMVOC's). These gaseous compounds have been known to inflict irreversible damage to the ozone layer, quality of life, environment and health [1]. Continuous monitoring and control of CO_2 using chemical sensors is important for process control in heavy industries such as power plants, chemical and metallurgical industries, petrol and diesel engine road vehicles (P-DERV), carbonation of concrete, food packaging, and environmental monitoring. CO_2 in particular is one of the main green-house gases, so called because it blocks light from re-radiating, thereby causing heat to be trapped which results in the warming up of the atmosphere. CO_2 contributes to the global warming by over 50% of the total gases that are responsible for global warming phenomenon.

Oxide ceramics are known to be chemically stable in harsh environments and therefore most of the research work on chemical sensors for more than two decades has been conducted using oxide ceramic materials. Gauthier and Chamberland [2] reported the first CO_2 sensor using gaseous electrodes and K_2CO_3 as a solid electrolyte. Since the publication of their research [2], there has been a large number of investigations [3–32] using variety of solid electrolyte materials such as alkali metal carbonates [2–7], beta-alumina [8–10, 12–14, 27], Nasicon [15–17, 19–26], stabilised-zirconia [31, 32] and Li-ion conducting electrolyte [28, 29, 33] for the development of a CO_2 sensor. A variety of reference and auxiliary electrode systems have been used in conjunction with an appropriate solid electrolyte with the aim of improving the response time, selectivity, stability of the sensor signal and manufacturing process. However, in almost all the earlier investigations, the CO_2 sensor tested by various group of investigators has been significantly bulky. Recent reports suggests that a thick and thin film gas sensing devices can be more reliable, could exhibit more stable response, will be less expensive to manufacture and can be easily integrated into microelectronic circuitry [34–37].

*Author to whom all correspondence should be addressed.

Therefore, in the present investigation we report the design and fabrication of solid state ceramic sensor for sensing CO_2 incorporating a bi-electrolyte couple consisting of a thin film of (8 mol% Y_2O_3) ZrO_2 (YSZ), an excellent O^{2-} anion conductor, on $Na_3Zr_2Si_2PO_{12}$ (Nasicon) substrate, a superionic Na^+ cation conductor, with Na_2CO_3 as an auxiliary electrode. The sensor has been based on the earlier work of Kale and Jacob [38] and is tested in the laboratory environment between 700 to 900 K. The main advantage of a bi-electrolyte sensor over a mono-electrolyte sensor is that the test gas is in contact with only one of the faces of the Nasicon solid electrolyte and hence there is no possibility of short-circuiting the two electrodes of the sensor. This has been explained in more details elsewhere by Kale *et al*. [39] for a bi-electrolyte SO_X sensor that has been successfully tested by Kale *et al*. [39] in the laboratory environment over a range of temperature and partial pressure of SO_2.

2. Experimental procedure

YSZ thin film was deposited on alumina and Nasicon substrate using a US-GUN-II radio frequency (RF) magnetron sputtering unit. Three different target materials such as high density YSZ disk, porous YSZ disk and fine powder of YSZ have been tested for fabricating thin film of YSZ. Both, high density YSZ and porous YSZ targets were found to crack during sputtering and hence the powder form of YSZ was used as sputtering target for rest of the investigation. The typical sputtering conditions are given in the Table I.

The thickness of thin film was measured by film thickness detector, which was mounted in the RF magnetron sputtering unit. The thin film of YSZ was sintered at 1300 K for 2 h. The formation of YSZ thin film on alumina and Nasicon substrate was confirmed by X-ray diffraction analysis. Cambridge S-250 MK3 equipped with EDX detector, capable of performing energy dispersive X-ray (EDX) analysis, was used to perform microstructural characterisation and elemental analysis. Ionic conductivity of sintered thin film of YSZ and dense pellet of YSZ was performed using SI-1260 frequency response analyser and controlled using Z-plot software. Platinum electrodes were attached to the surface of YSZ thin film by painting Pt-ink (Engelhardt A4731) and firing the surface at 1173 K for 10 min. Pt wires were attached to the two electrodes through the spot welded Pt-gauze.

The CO_2 sensor was fabricated by coating Pt electrodes on both sides of the bi-electrolyte couple using Pt-ink (Engelhardt A4731) and firing the structure at 1173 K for 10 min. Pt wires were attached to the two electrodes through the Pt-gauze. An auxiliary electrode consisting of Na_2CO_3 thick film was attached on surface of Nasicon by painting a saturated solution of Na_2CO_3 and heating the structure at 398 K until dry Na_2CO_3 was deposited on the Nasicon surface. The final structure of the YSZ thin film for ac-conductivity measurement and the CO_2 sensor is schematically shown in Fig. 1. The CO_2 sensor can be schematically written as follows:

TABLE I Optimum sputtering conditions for fabrication of thin film of YSZ

Working gas	99% Argon
Gas pressure	5×10^{-3} Torr
RF power	200–300 W
Substrate used	Nasicon, Alumina and Silca
Substrate temperature	298 K
Distance between target and substrate	14 cm
Sputtering target	YSZ powder

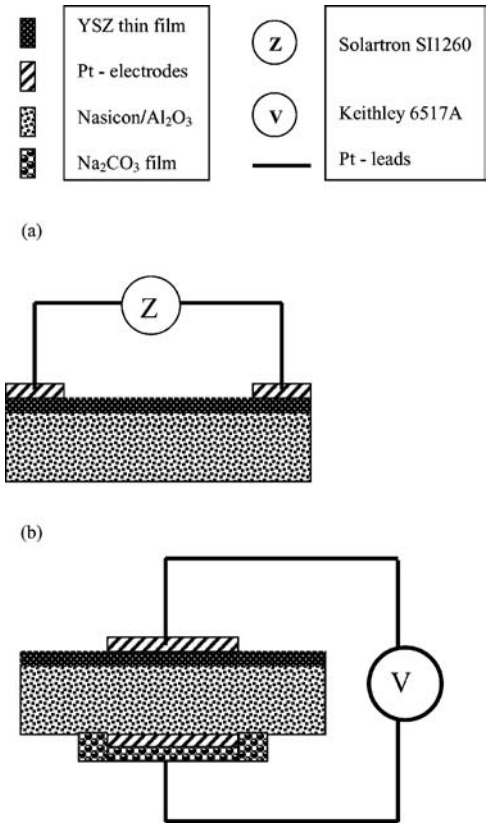

Figure 1 Schematic diagram of (a) structure for ac-conductivity measurement of YSZ thin film (b) structure of a bi-electrolyte CO_2 sensor.

$$CO_2, O_2 \mid Na_2CO_3 \mid Pt \mid \text{Nasicon pellet} \mid \text{YSZ thin film} \mid Pt, O_2, CO_2 \quad \text{(I)}$$

According to Kale and Jacob [38], the anodic reaction at Na_2CO_3/Nasicon interface is:

$$\text{Anodic reaction: } Na_2CO_3(s) \rightarrow 2Na^+ + 1/2O_2(g) + CO_2(g) + 2e^- \quad (1)$$

And the cathodic reaction at the YSZ/O_2 interface is:

$$\text{Cathodic reaction: } 1/2O_2(g) + 2e^- \rightarrow O^{2-} \quad (2)$$

Therefore, the reaction at the interface between Nasicon and YSZ is:

$$\text{Interfacial reaction: } 2Na^{2+} + O^{2-} \rightarrow Na_2O_{\text{Nasicon}}(s) \quad (3)$$

The partial pressure of oxygen at both the electrodes is equal and therefore, combining reactions (1-3) gives the overall chemical reaction for the CO_2 sensor described by cell (I) as follows:

$$\text{Overall reaction: } Na_2CO_3(s) \rightarrow Na_2O_{Nasicon}(s) + CO_2(g) \quad (4)$$

For a Nernstian electrochemical sensor, the emf of the CO_2 sensor can be related to the partial pressure of CO_2 in the gas mixture according to the equation:

$$-nFE = \left[\Delta G^{o}_{Na_2O} + \Delta G^{o}_{CO_2} - \Delta G^{o}_{Na_2CO_3}\right] + RT\ \mathrm{Ln}\left[\left(a_{Na_2O} \cdot P_{CO_2}\right)/a_{Na_2CO_3}\right] \quad (5)$$

where n is the number of electrons participating in the electrode reaction of cell (I), F is the Faraday constant, E is the emf of the CO_2 sensor in V and P is the partial pressure of CO_2in the gas mixture. Assuming that the thermodynamic activity of Na_2CO_3 at the auxiliary electrode is unity, and rearranging Equation. 5 gives:

$$E = 1/nF\left[-\Delta G^{o}_{4} - RT\ \mathrm{Ln}\left(a_{Na_2O} \cdot P_{CO_2}\right)\right] \quad (6)$$

The partial thermodynamic properties of Na_2O (ΔH_{Na_2O} and ΔS_{Na_2O} and ΔG_{Na_2O}) in Nasicon solid solution series have been measured employing solid-state electrochemical technique by Kale and Jacob [38]. It can be easily seen that at a fixed temperature and composition of Nasicon solid solution, Equation 6 transforms to:

$$E = A - B\ \mathrm{Log}\ P_{CO_2} \quad (7)$$

where A and B are constant.

The emf measurements were carried out over a range of temperature between 700 and 900 K. The gas mixtures of CO_2 and synthetic air with CO_2 concentration varying from 1 to 100% were prepared by mixing CO_2 and air using mass-flow controllers. The flow rate of measuring gas was maintained at 100 cm^3 min^{-1}. The open circuit emf of the CO_2 sensor was measured using a Keithley 6517A high impedance ($>10^{12}$ Ω) multi channel digital electrometermeter. A detailed experimental set-up is shown elsewhere [39].

3. Results and discussion

3.1. Deposition and characterisation of YSZ thin film

YSZ thin film was deposited on surface of two different substrates, high density Al_2O_3 and Nasicon ($Na_3Zr_2Si_2PO_{12}$), under different conditions in order to optimise the deposition conditions to produce crack free thin film of YSZ. The optimum conditions required to produce a crack free thin film approximately 1.5 μm thick are given in Table I. The thickness of the film could be increased up to 6 μm by multiple sputtering. The as sputtered YSZ thin film was found to be light yellow in colour. After heat treating the deposited thin film of YSZ at more than 1300 K, the YSZ film became dense, transparent and the bonding between the film and substrate improved significantly. The X-ray diffraction pattern of YSZ thin film as prepared on alumina substrate is shown in Fig. 2a and after heat treating the film at 1300 K for 2 h is shown in the Fig. 2b.

The Fig. 2a and b confirm that the YSZ thin film has formed on surface of alumina substrate. The thickness of film was found to be approximately 1.5 μm and therefore the diffraction peaks of Al_2O_3 are seen in the X-ray diffraction pattern of YSZ thin film deposited on alumina substrate. The appearance of diffraction peaks of as sputtered YSZ film shows that the film was crystalline and not amorphous as expected by sputtering at ambient temperature although the peaks are not sharp because of fine grain size (Fig. 2a). After the YSZ film was treated at 1300 K for 2 h, the intensity of peak increased and the width of the peak decreased rendering the peaks more sharper (Fig. 2b). The diameter of grains in YSZ thin film can be estimated by the broadening of the X-ray peaks as described by Jacob *et al*. [37] for nano-crystalline $MgAl_2O_4$ spinel powders and for nano-crystalline $ZnFe_2O_4$ spinel thin film by Tanaka *et al*. [40] using the Scherrer's equation given as follows:

$$D = 0.9\lambda/\beta\ \mathrm{Cos}\,\theta \quad (8)$$

where D is the average diameter of grain, β is the width of the most intense XRD peak in radians at full width-half maxima, λ is the Cu-K_α wavelength equal to 0.15418 nm and θ is the Bragg angle. Assuming that the YSZ thin film deposited by RF-sputtering is stress free, the calculations using Equation 8 gives the average grain diameter of as sputtered YSZ film approximately equal to 7 (±5) nm. The average grain diameter in YSZ thin film after heat treating at 1300 K for 2 h has been calculated as approximately equal to 12 (±5) nm using Equation 8.

The scanning electron micrographs of YSZ thin film on Nasicon substrate after heat treating at 1300 K for 2 h is shown in Figs 3 and 4. It can be seen in Fig. 3a that after the first run of sputtering and heat treating the YSZ film is not uniformly dense and also it shows wide cracks mainly originating from the areas that have lower mass distribution due to the uneven material flow during the heat treatment process. However the cracks could be bridged by multiple sputtering and heat treating sequences as shown in Fig. 3b. The SEM micrograph of a fractured cross section of Nasicon-YSZ thin film composite, as seen in Fig. 4, indicates that the YSZ film is strongly bonded to Nasicon surface and also that the YSZ thin film is crack free. A crack free YSZ thin film is an important feature of the bi-electrolyte for designing a CO_2sensor. In addition to this, the cross-sectional view of the bi-electrolyte shown in Fig. 4 indicates that there are some disconnected pores across the thickness of the Nasicon substrate. We believe that these pores are formed either due to pull out of grains during the polishing of the cross-section of the bi-electrolyte or they are formed as a result of insufficient densification of Nasicon substrate. The porosity of Nasicon substrate was less than 3% and hence the observed porosity may not have any significant influence on the performance

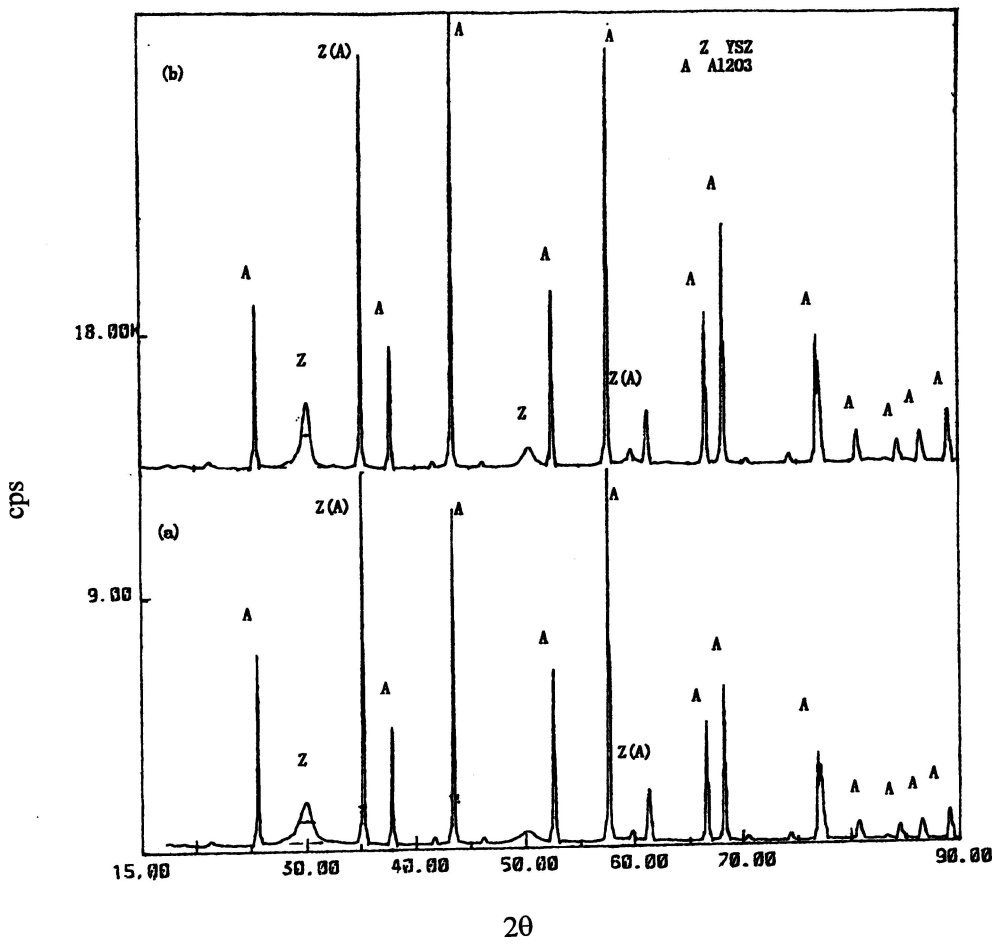

Figure 2 XRD pattern of YSZ thin film (a) as sputtered on Al_2O_3 substrate and (b) after heat treating at 1300 K for 2 h.

of the sensor. The elemental composition of YSZ thin film determined by EDX analysis was found to be 20.88 at.% of Y and 78.69 at.% Zr which is in excellent agreement with the theoretical composition of 8 mol% Y_2O_3 stabilised ZrO_2.

3.2. Conductivity of YSZ thin film

Ac-conductivity of YSZ thin film and dense pellet has been measured over a range of frequency between 10 Hz to 10 MHz as a function of temperature. Typical complex impedance diagrams of YSZ thin film as a function of temperature between 723–923 K are shown in Fig. 5. Similar complex impedance diagrams were obtained for a sintered high density YSZ pellet. The data shown in Fig. 5 was fitted using Z-view software to determine the conductivity of YSZ thin film and similar procedure was adopted for the dense pellet as well. The logarithm of the conductivity of YSZ thin film is plotted as a function of reciprocal of absolute temperature in Fig. 6 in comparison with the conductivity of bulk YSZ pellet. The variation of the logarithm of ionic conductivity with the reciprocal of absolute temperature is in agreement with the Arrhenius equation, $\sigma T = \sigma^{\circ} Te^{(-E_a/\mathrm{kT})}$ where σ is the conductivity in Scm^{-1}, σ° is a pre-exponential constant, E_a is the activation energy for ionic motion in eV, k is the Boltzman costant and T is the absolute temperature. The activation energy for ionic conduction in YSZ thin film has been calculated as 0.98 eV that agrees well with the values ranging between 0.86 and 1.04 eV for YSZ bulk material reported in the literature [42–45]. It is interesting to note that the conductivity of the YSZ film has been found to be greater than that of YSZ pellet by approximately half an order of magnitude over the entire range of temperature as is seen in Fig. 6. This is probably because the YSZ thin film has grain size approximately 12 ($\pm$5) nm whereas the dense pellet has a grain size of approximately 500 nm–1.5 μm [46] and it has been shown that the nano-structured ceramics have improved electrical properties compared to the bulk ceramics [47].

3.3. Testing of CO_2 sensor

The response transient of the planar thin film sensor for sensing CO_2 is shown in Fig. 7, which is similar to that obtained for a tube type CO_2 sensor [26]. The response of CO_2 sensor in this investigation has been found to be significantly rapid compared to the tube type sensor tested by Kale *et al.* [26]. A 95% of the response (t_{95}) of the CO_2 sensor tested in this investigation was found to be approximately 200 s compared to 720 s for a tube type CO_2 sensor [26]. The variation of the sensor emf with time was also monitored for more than 3 h at a fixed concentration and it was found that the sensor emf remained stable with in $\pm$3 mV of the equilibrium value at all the CO_2 concentrations and temperature of measurement. Fig. 7 clearly indicates that the response of the CO_2 sensor is reproducible at all the concentrations of CO_2 at a fixed temperature.

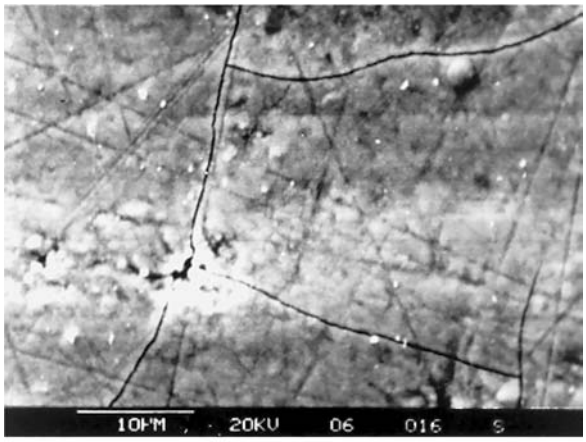

(a)

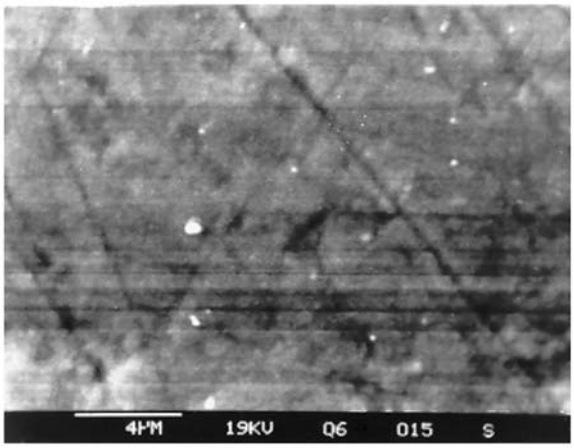

(b)

Figure 3 SEM micrograph of YSZ thin film sputtered on Nasicon substrate (a) single sputtering followed by heat treatment at 1300 K for 2 h, (b) multi-sputtering followed by heat treatment at 1300 K for 2 h.

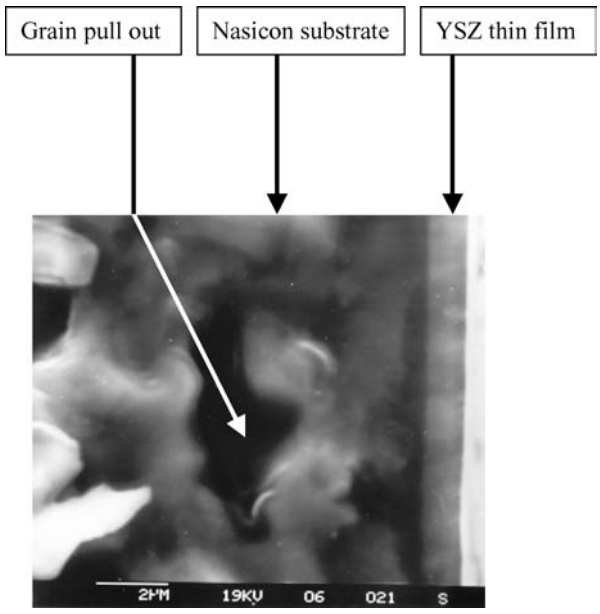

Figure 4 Cross-sectional view of a fractured YSZ thin film on Nasicon substrate under SEM.

The variation of the open circuit emf of the CO_2 sensor as a function of concentration of CO_2 in the gas mixture is shown in Fig. 8 at 800 and 900 K. The variation of emf with the logarithm of the partial pressure of CO_2 has been found to be a linear and follows a Nernstian be-

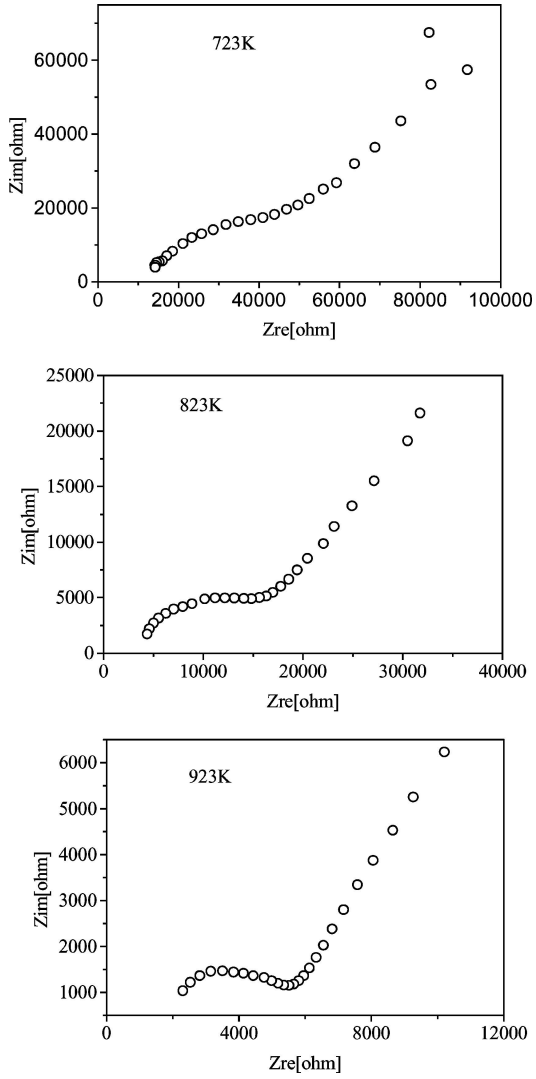

Figure 5 Complex impedance diagram of YSZ thin film at different temperatures.

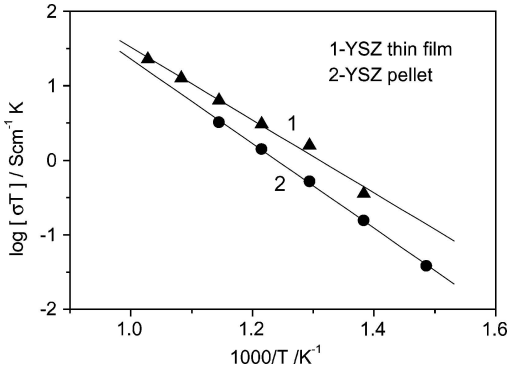

Figure 6 Comparison of the temperature dependence of electrical conductivity of YSZ thin film and pellet.

haviour given by the Equation 7. A least squares regression analysis of the measured data shown in Fig. 8 gives the slope of the linear segment equal to 81.3 and 90.5 mV/decade at 800 and 900 K, respectively. The equivalent number of electrons transferred in the external circuit due to the electrochemical reactions at cathode and anode of cell (I) can be easily calculated from the slope of linear segments in Fig. 8 using Equation 6. The calculated value of 1.95 and 1.97 at 800 and 900 K, respectively is in excellent agreement with the theoretical

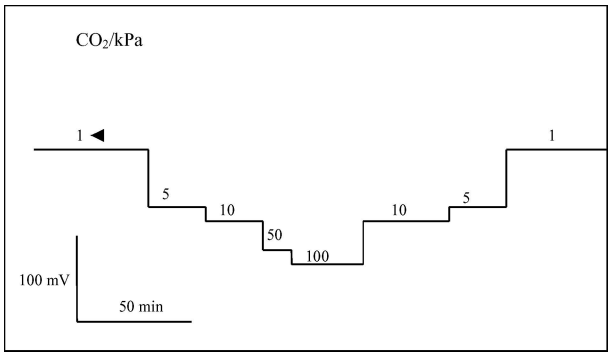

Figure 7 Response transient of a typical planar CO_2 sensor at 900 K. The numbers on the plateau indicate the concentration of CO_2 in kPa.

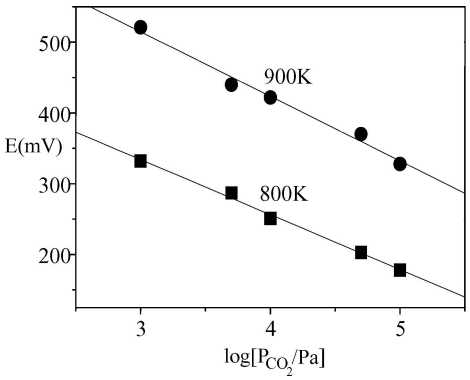

Figure 8 Variation of the open circuit emf of CO_2 sensor as a function of the partial pressure of CO_2 at 800 and 900 K.

value of 2 used in Equation 6. This clearly suggests that the CO_2 sensing measurements performed in the present investigation using a CO_2 sensor based on Nasicon/YSZ thin film bi-electrolyte are thermodynamically consistent and that the bi-electrolyte CO_2 sensor exhibits Nernstian behaviour.

4. Conclusion

The YSZ thin film has been fabricated on Nasicon and Al_2O_3 substrates by using RF magnetron sputtering and the effect of processing conditions on the microstructure and ionic conductivity have been studied. The results indicate that the film is dense, crack-free and strongly bonded to substrate after it is treated at 1300 K for 2 h. The average grain diameter of sintered YSZ thin film is found to be 12 ($\pm$5) nm. The conductivity of sputtered YSZ thin film is approximately half an order of magnitude higher than that of sintered pellet however the activation energy for ionic motion was nearly the same. The response of planar thin film type of CO_2 gas sensor based on YSZ thin film on Nasicon substrate was found to be Nernstian. The 95% of the equilibrium emf value of the CO_2 sensor could be attained within approximately 200 s.

Acknowledgement

Financial support for Dr. L. Wang from the Royal Society (UK) grant Q737 awarded to Dr. Kale is gratefully acknowledged. Authors also wish to thank the National Natural Science Foundation of China for supporting the work under grant No. 59582004.

References

1. J. W. L. GOODWIN, A. G. SALWAY, T. P. MURRELLS, C. J. DORE, N. R. PASSANT and H. S. EGGLESTON, "UK Emissions of Air Pollutants 1970–1998" (Department of the Environment, Transport and the Regions, London, 2000).
2. M. GAUTHIER and A. CHAMBERLAND, *J. Electrochem. Soc.* **124** (1977) 1579.
3. R. COTE, C. BALE and M. GAUTHIER, *ibid.* **131** (1984) 63.
4. H. NARITA, Z. Y. CAN, J. MIZUSAKI and H. TAGAWA, *Solid State Ion.* **79** (1995) 349.
5. A. DUBBE, H. D. WIEMHOFER, Y. SADAOKA and W. GOPEL, *Sensors and Actuators B* **25** (1995) 600.
6. A. DUBBE, H. D. WIEMHOFER and Y. SADAOKA, *J. Electrochem. Soc.* **144** (1997) 943.
7. A. DUBBE, M. WAKE and Y. SADAOKA, *Solid State Ion.* **96** (1997) 201.
8. M. HOLZINGER, J. MAIER and W. SITTE, *ibid.* **86–88** (1996) 1055.
9. *Idem.*, *ibid.* **94** (1997) 217.
10. J. MAIER and U. WARHUS, *J. Chem. Thermodyn.* **18** (1986) 309.
11. J. MAIER, *Solid State Ion.* **62** (1993) 105.
12. J. MAIER, M. HOLZINGER and W. SITTE, *ibid.* **74** (1994) 5.
13. J. LIU and W. WEPPNER, *Solid State Comm.* **76** (1990) 311.
14. G. HE, T. GOTO, T. NARUSHIMA and Y. IGUCHI, *Solid State Ion.* **121** (1999) 313.
15. T. MARUYAMA, S. SASAKI and Y. SAITO, *ibid.* **23** (1987) 107.
16. T. MARUYAMA, X.-Y. YE and Y. SAITO, *ibid.* **23** (1987) 113.
17. *Idem.*, *ibid.* **24** (1987) 281.
18. Y. SAITO and T. MARUYAMA, *ibid.* **28–30** (1988) 1644.
19. N. MIURA, S. YAO, Y. SHIMIZU and N. YAMAZOE, *J. Electrochem. Soc.* **139** (1992) 1384.
20. Y. SADAOKA, M. MATSUGUCHI, Y. SAKAI and D. MANABE, *J. Mater. Sci.* **28** (1993) 2035.
21. Y. SADAOKA, Y. SASAKI and T. MANABE, *Sensors and Actuators B* **15** (1993) 166.
22. V. LEONHARD, D. FISCHER, H. ERDMAN, M. ILGENSTEIN and H. KOPPEN, *ibid.* **14** (1993) 530.
23. D. LEE, S. CHOI and K. LEE, *ibid.* **25** (1995) 607.
24. K. KANEYASU, K. OTSUKA, Y. SETOGUCHI, S. SONODA, T. NAKAHARA, I. ASO and N. NAKAGAICHI, *ibid.* **66** (2000) 56.
25. S. SALAM, S. BREDIKHIN, P. BIRKE and W. WEPPNER, *Solid State Ion.* **110** (1998) 319.
26. G. M. KALE, A. J. DAVIDSON and D. J. FRAY, *ibid.* **86–88** (1996) 1107.
27. H. NAFE and F. ALDINGER, *Sensors and Actuators B* **69** (2000) 46.
28. N. IMANAKA, T. MURATA, T. KAWASATA and G. ADACHI, *ibid.* **13** (1993) 476.
29. N. IMANAKA, Y. HIROTA and G. ADACHI, *ibid.* **25** (1995) 380.
30. Y. SADAOKA, S. NAKAYAMA, Y. SAKAI and M. WAKE, *ibid.* **24** (1995) 282.
31. T. SUGAI and T. MATSUZAWA, *ibid.* **13** (1993) 480.
32. N. MIURA, Y. YAN, M. SATO, S. YAO, S. NONAKA, Y. SHIMIZU and N. YAMAZOE, *ibid.* **25** (1995) 260.
33. C. H. LEE, S. A. AKBAR and C. O. PARK, *ibid.* **80** (2001) 234.
34. L. WANG and R. V. KUMAR, *Solid State Ion.* **158** (2003) 309.
35. T. LANG, H. D. WIEMHOFER and W. GOPEL, *Sensors and Actuators B* **34** (1996) 383.
36. N. SZABO, C. LEE, J. TRIMBOLI, O. FIGUEROA, R. RAMAMOORTHY, S. MIDLAM-MOHLER, A. SOLEMAN, H. VERWEIJ, P. K. DUTTA and S. A. AKBAR, *J. Mater. Sci.* **38** (2003) 4239.

37. B. J. WARD, C. C. LIU and G. W. HUNTER, *ibid.* **38** (2003) 4289.
38. G. M. KALE and K. T. JACOB, *J. Mater. Res.* **4** (1989) 417.
39. G. M. KALE, L. WANG and Y. R. HONG, *Solid State Ion.* **161** (2003) 155.
40. K. T. JACOB, K. P. JAYADEVAN, R. M. MALLAYA and Y. WASEDA, *Adv. Mater.* **12** (2000) 440.
41. K. TANAKA, S. NAKASHIMA, K. FUJITA and K. HIRAO, *J. Phys. Condens. Matter.* **15** (2003) L469.
42. M. FUKUYA, K. HIROTA, O. YAMAGUCHI, H. KUME, S. INAMURA, H. MIYAMOTO, N. SHIOKAWA and R. SHIKATA, *Mater. Res. Bull.* **29** (1994) 619.
43. B. Y. LIAW and W. WEPPNER, *J. Electrochem. Soc.* **138** (1991) 2478.
44. S. P. S. BADWAL, F. T. CIACCHI and D. V. HO, *J. Appl. Electrochem.* **21** (1991) 721.
45. R. KURCHANIA and G. M. KALE, *J. Mater. Res.* **15** (2000) 1576.
46. G. M. KALE, L. WANG, J. E. HAYES, J. CONGJIN and Y. R. HONG, *J. Mater. Sci.* **38** (2003) 4293.
47. Y. W. ZHANG, Y. YANG, S. JIN, S. J. TIAN, G. B. LI, J. T. JIA, C. S. LIAO and C. H. YAN, *Chem. Mater.* **13** (2001) 372.

Received 17 October 2003
and accepted 14 October 2004